

Chapter 4

H α profile variations in the long-period Cepheid ℓ Carinae

The content of this chapter was published in paper Baldry et al. (1997) in collaboration with Melinda Taylor, Tim Bedding and Andrew Booth. I wrote the paper and reduced the data with the supervision of T. Bedding. M. Taylor did most of the observing (see Table 4.1) with help from A. Booth.

4.1 Introduction

ℓ Carinae is the brightest classical Cepheid in the southern sky. It will be a primary target for the Sydney University Stellar Interferometer (SUSI) as part of a programme for measuring the angular diameter of Cepheids (Booth et al. 1995), and much work is being done to improve the general understanding and the radial velocity curve of this star (Taylor et al. 1997). Here we present spectra showing what appears to be continuous $H\alpha$ emission throughout the whole pulsation cycle in ℓ Car. In long-period Cepheids the $H\alpha$ line has often shown two components in absorption but only sometimes shown an emission feature (Rodgers & Bell 1968; Wallerstein 1972, 1983). We believe that the true shape and flux of the emission in ℓ Car are largely obscured by upper atmospheric and circumstellar absorption as occurs with Mg II emission (Böhm-Vitense & Love 1994). The origin of the emission feature may be a shock front in the atmosphere of the star or may be the upper atmosphere (we avoid the term chromosphere: see the discussion by Sasselov & Lester 1994).

From the early work on the $H\alpha$ line in Cepheids (Wallerstein 1972), it appears that in stars with periods less than about 13 days the $H\alpha$ line behaves more or less like other absorption lines. Anomalous $H\alpha$ profiles have been observed in many long-period Cepheids (Grenfell & Wallerstein 1969; Schmidt 1970) and it is generally agreed that the photospheric line is largely obscured by upper atmospheric absorption and emission in these stars. However Schmidt (1970) argued that the wings of $H\alpha$ could be used as an effective temperature indicator as long as the measurements of the width of the line are made far enough away from the upper atmospheric core. Our original aim was to measure the equivalent width of $H\alpha$ in ℓ Car as a function of phase but this has not been possible with our data set.

ℓ Car (HR 3884, HD 84810) has $\langle V \rangle = 3.7$, full range $\Delta V = 0.7$, $\langle B - V \rangle = 1.2$ and a spectral type around G5Iab. We adopt a period of 35.54434 days and a zero-phase (maximum light) Julian date of 2447880.81 (Shobbrook 1992). The period is known to vary but not enough to affect the results in this chapter.

We use photometric phases referenced to maximum light. In order to convert to a more physically related phase it is best to define zero phase to be minimum radius, which occurs at photometric phase 0.93 in this star (i.e. add 0.07 to all the phases quoted in this chapter).

4.2 Observations and data reductions

We obtained high-resolution optical spectra of ℓ Carinae at Mount Stromlo Observatory, with the 1.88-m telescope and coude echelle spectrograph, between February 1994 and April 1995. A single spectrum contained about 45 orders, each approximately 100Å long, projected on to a 2K Tek CCD. The dispersion was $\sim 0.05\text{Å}$ per pixel and the full width at half maximum of the instrumental profile was $\sim 0.10\text{Å}$. Moderately full phase coverage of ℓ Car was obtained (the largest gap in the coverage is 0.085 of a cycle between phases 0.609 and 0.694). Table 4.1 provides a list of the dates and phases of the 33 spectra analysed for this paper.

The data were reduced using the FIGARO software package (Shortridge 1993). For the purposes of this chapter only the two orders containing $H\alpha$ were reduced. Other work has been done on the radial velocities of metal lines by Taylor et al. (1997) using more of the orders.

The reduction began with bias subtraction followed by extraction of orders. Corrections using the flat fields were not applied to the data as they were not useful either for tracing the shape of the order or for correcting pixel-to-pixel variations on the CCD. This was because the two orders around $H\alpha$ were in a vignetted part of the CCD, such that the flat field and the star profiles were significantly different and there were not enough photons in the combined flat field images to reduce the photon noise below the level of the pixel-to-pixel variations on the CCD. Once the orders were extracted, the white scattered light level was removed by using an estimate obtained from levels either side of the star light. Cosmic rays were removed by interpolating across that part of the spectrum. The spectra from the 29th March to the 10th April 1995 contained some high-frequency pattern noise which was reduced significantly by smoothing using a three-point triangle (0.25,0.50,0.25). This smoothing was applied to all 33 spectra to ensure consistency. In most cases no pattern noise was left, an exception being the data from the 1st April (see Figure 4.1, phase 54.244). Finally a pseudo-continuum was fitted to each spectrum and wavelengths were calibrated using arc spectra. The ‘continuum fitting’ was the most critical part of the data reduction and was done by eye, aiming to get a good fit over the region of the order 13Å either side of the $H\alpha$ core at 6563Å . It is not possible to analyse the depth of the wings of $H\alpha$ using this set of data because of the difficulty of obtaining a good continuum fit over a region much larger than 26Å . In fact the wings will have been removed by our fitting procedure.

Table 4.1 Log of the observations of ℓ Car

Date	UT	Observer	JD -2449000	Phase
1994 Feb 25	13.7	P.R.Wood	409.07	42.996
1994 Feb 26	11.3	P.R.Wood	409.97	43.021
1994 Feb 28	10.3	P.R.Wood	411.93	43.076
1994 Mar 01	12.1	P.R.Wood	413.00	43.106
1994 Mar 02	10.4	P.R.Wood	413.93	43.133
1994 Mar 29	10.0	P.R.Wood	440.92	43.892
1994 Mar 31	11.1	H.M.Schmidt	442.96	43.949
1994 Jun 27	08.2	M.M.Taylor	530.84	46.422
1994 Jun 28	07.7	M.M.Taylor	531.82	46.449
1994 Jun 29	08.2	M.M.Taylor	532.84	46.478
1994 Jul 09	08.9	M.M.Taylor	542.87	46.760
1994 Jul 10	08.2	M.M.Taylor	543.84	46.787
1994 Jul 11	08.7	M.M.Taylor	544.86	46.816
1994 Jul 12	08.6	M.M.Taylor	545.86	46.844
1994 Jul 13	07.8	M.M.Taylor	546.82	46.871
1994 Jul 14	07.9	M.M.Taylor	547.83	46.900
1995 Mar 29	11.6	M.M.Taylor	805.98	54.163
1995 Mar 31	08.7	M.M.Taylor	807.86	54.215
1995 Apr 01	08.7	M.M.Taylor	808.86	54.244
1995 Apr 02	09.0	M.M.Taylor	809.88	54.272
1995 Apr 03	08.8	M.M.Taylor	810.87	54.300
1995 Apr 04	09.1	M.M.Taylor	811.88	54.328
1995 Apr 05	08.7	M.M.Taylor	812.86	54.356
1995 Apr 08	13.4	M.M.Taylor	816.06	54.446
1995 Apr 10	11.7	M.M.Taylor	817.99	54.500
1995 Apr 11	08.7	M.M.Taylor	818.86	54.525
1995 Apr 12	09.1	M.M.Taylor	819.88	54.554
1995 Apr 13	09.2	M.M.Taylor	820.88	54.582
1995 Apr 14	08.7	M.M.Taylor	821.86	54.609
1995 Apr 17	08.6	M.M.Taylor	824.86	54.694
1995 Apr 18	08.4	M.M.Taylor	825.85	54.722
1995 Apr 19	11.6	M.M.Taylor	826.98	54.753
1995 Apr 20	08.7	M.M.Taylor	827.86	54.778

4.3 The $H\alpha$ profiles

The $H\alpha$ profiles are plotted in Figures 4.1–4.4 over the range 6550Å to 6576Å (heliocentric wavelength) and are normalised so that the continuum is at approximately 1.0, except that each plot is offset from the previous one by a factor equal to ten times the phase difference. The spectra are plotted from top to bottom in each figure in order of phase, but note that the observations span several cycles.

There is some repetition in the phase coverage from cycle to cycle, for instance the data from the 28th June 1994 and the 8th April 1995 are almost at the same phase. There are four pairs of spectra with a phase difference of less than 0.010 (43.892 & 46.900, 46.449 & 54.446, 46.760 & 54.753, 46.787 & 54.778). There are slight differences between the profiles from cycle 47 and from 55 but we suggest they are caused by the changing strength and position of the terrestrial atmospheric lines. We see no significant cycle to cycle variations in the $H\alpha$ profile in ℓ Carinae during 1994 and 1995. Taylor et al. (1997) discuss variations from cycle to cycle in the radial velocities of metal lines.

Throughout the whole pulsation cycle, there is a dominant absorption component (6562.9Å) whose velocity ($+4 \text{ km s}^{-1}$) appears to be constant. This means that it does not partake in the pulsation and we attribute this component to a circumstellar shell; this was also seen by Rodgers & Bell (1968). Mass loss (Deasy 1988) from the star is the probable origin for the circumstellar material. There must also be at least one other absorption component and an emission component to explain the complexity of the profile at different phases. The radial velocities of the non-constant components are difficult to measure due to blending effects.

From phase 0.1 (just after maximum light) to phase 0.4 there is an obvious red-shifted emission component of $H\alpha$. The spectrum from phase 0.106 also shows more possible absorption components at 6561.8Å and at 6563.7Å. The latter feature is possibly caused by a weak terrestrial line (rest wavelength 6563.521Å). Alternatively this profile could be caused by a very weak emission feature not related to the redward emission. These weak features have disappeared by phase 0.244, leaving a P-Cygni-like profile. From phase 0.4 we see a weakening of the redward emission and by phase 0.500 (minimum light) it has disappeared. At this point there may be a very weak blueward emission component but this is not convincing due to the possibility of the line Si I (rest wavelength 6560.6Å) becoming stronger and creating this profile. However the blueward emission grows stronger (see Figure 4.3) and by phase 0.844 it is clearly present. Figure 4.4 shows the sudden decrease in the blueward emission from phase 0.892 to 0.996. Then from maximum light onwards the cycle starts again with an increase in the redward emission.

During the phases around maximum light (see Figure 4.4) there is evidence of absorption line doubling, as has been seen in other Cepheids (Grenfell & Wallerstein 1969; Wallerstein 1972, 1983) but there is also possible contamination with terrestrial lines. The weak nature of this effect in ℓ Car is consistent with significant absorption line doubling from the upper atmosphere, which has been mostly obscured by circumstellar absorption.

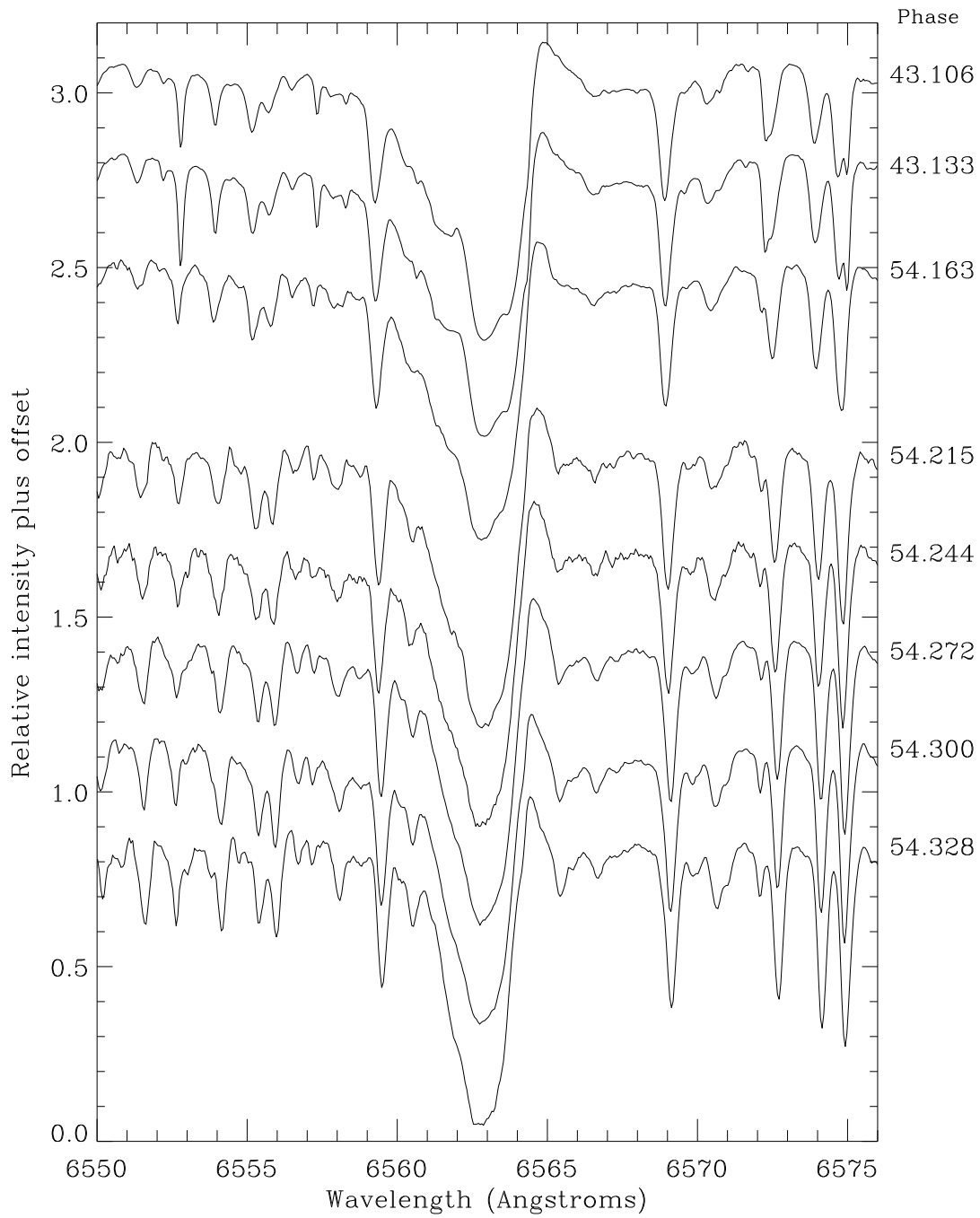


Figure 4.1 Plots of the $H\alpha$ profile in ℓ Car when the emission is redward of the central absorption

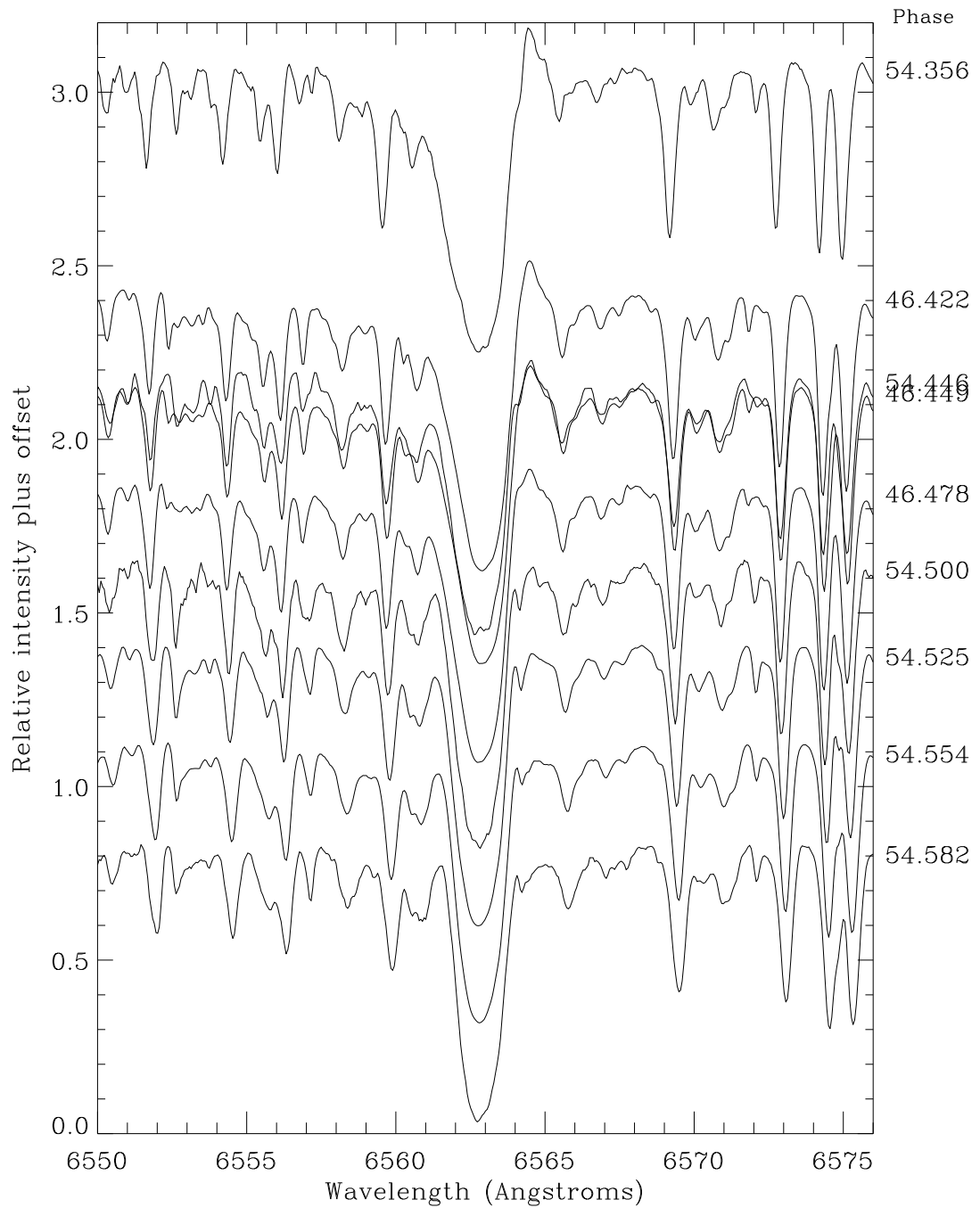


Figure 4.2 Plots of the $H\alpha$ profile in ℓ Car during the change from redward to blueward emission

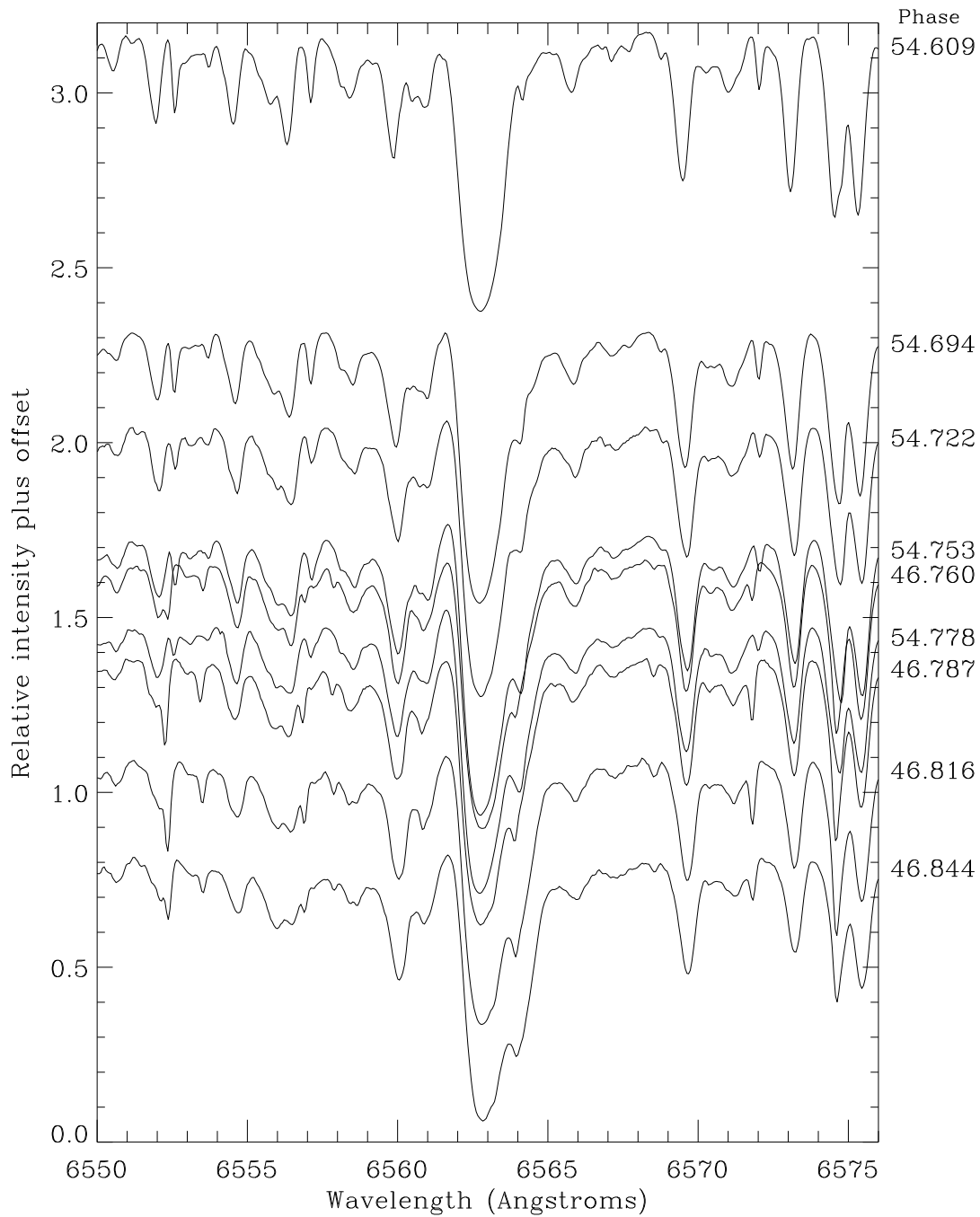


Figure 4.3 Plots of the $H\alpha$ profile in ℓ Car when the emission is blueward of the central absorption

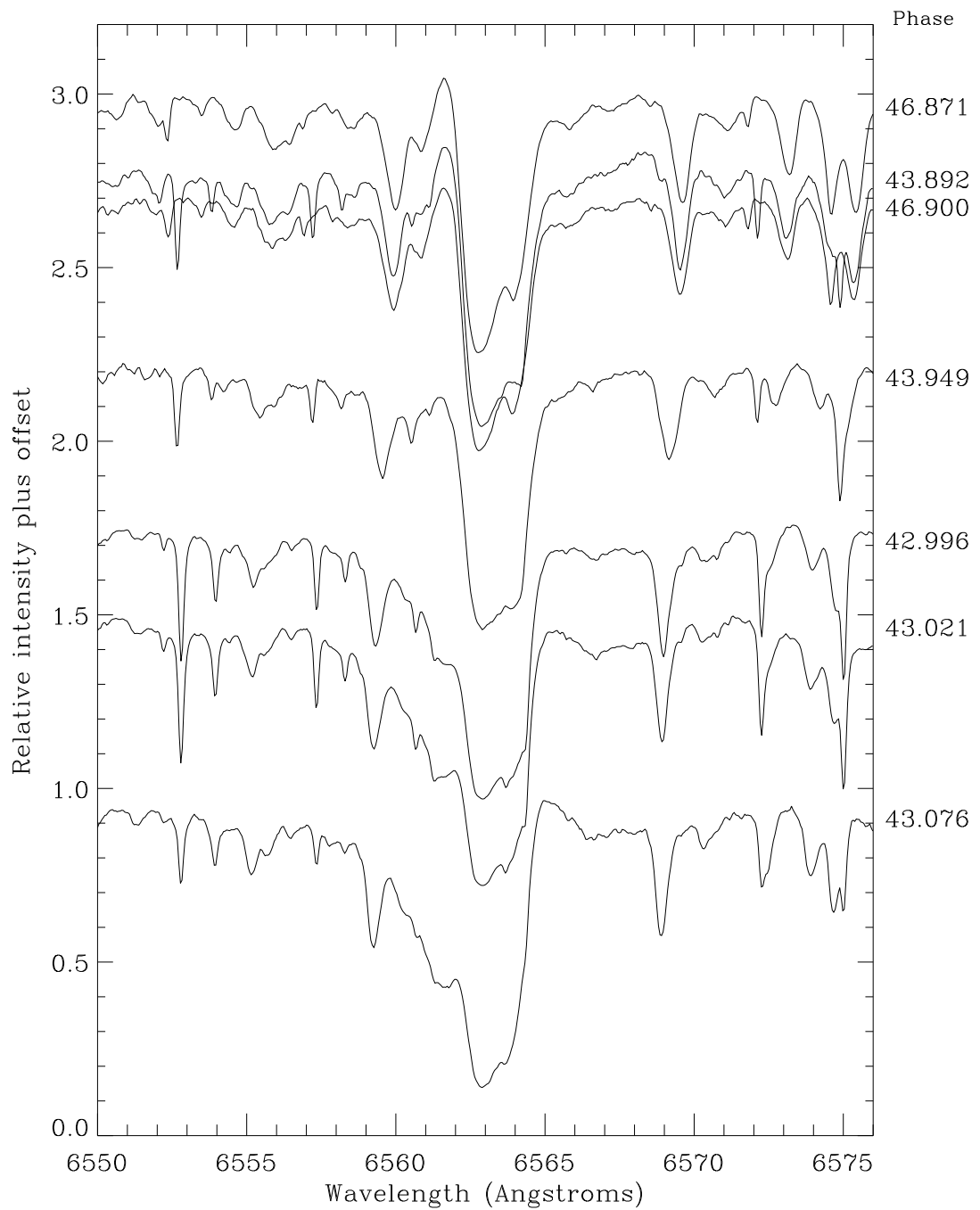


Figure 4.4 Plots of the $H\alpha$ profile in ℓ Car during the change from blueward to redward emission

4.4 Discussion

$H\alpha$ emission is seen in other yellow supergiants (Sowell 1990; Mallik 1993) and not just in long-period Cepheids. Sowell (1990) observed $H\alpha$ emission in 13 out of 40 stars in his survey and several other stars had possible weak emission features. Mass flows and circumstellar shells are invoked to explain some of the distorted $H\alpha$ profiles in these stars. For photometrically variable supergiants there are also pulsation and shock mechanisms capable of producing asymmetrical profiles. This makes it difficult to determine the cause of the observed $H\alpha$ emission in Cepheids because one cannot easily distinguish between a generic supergiant phenomenon, where the emission is constant but the profile changes due to blending effects with an absorption component, and a pulsation phenomenon where the emission actually changes throughout the cycle.

Barrell (1978) discovered a surprisingly high frequency and strength of $H\alpha$ emission components in beat Cepheids, which are classical Cepheids having more than one mode of pulsation. She suggested that the emission may indicate the existence of an acoustically heated upper atmosphere surrounding beat Cepheids. She (Barrell 1981) later made measurements of the effective temperatures of some beat Cepheids as a function of phase by using the width of the $H\alpha$ line. This was possible because the emission in the beat Cepheids was not present most of the time and if present was not usually strong enough to affect measurements using the wings of the $H\alpha$ line.

There have been several studies of $H\alpha$ behaviour in classical Cepheids (Bell & Rodgers 1967; Rodgers & Bell 1968; Grenfell & Wallerstein 1969; Schmidt 1970; Wallerstein 1972, 1979, 1983; Jacobsen & Wallerstein 1982; Wallerstein et al. 1992). In a few cases $H\alpha$ emission has been observed but only on the red wing and only for a fraction of the pulsation cycle. Wallerstein (1972) suggested that a small red emission feature in T Mon is due to broad emission which is largely self-absorbed, leaving a small sharp red wing. The strong emission could be caused by shock heating.

Gillet et al. (1994) have observed BL Her, a Population II Cepheid. They observed a small sharp blue wing in $H\alpha$ emission in phases 0.82 and 0.86 and absorption line doubling before and after maximum light. This is similar to what might be happening in ℓ Carinae between phases 0.8 and 0.2 except that the circumstellar material is obscuring the effect. Fokin & Gillet (1994) model the $H\alpha$ profile in BL Her in terms of shock wave propagation in an extended atmosphere. We have to be careful about comparing BL Her and ℓ Car because of the difference in periods, 1.3 days and 35.5 days respectively.

Now we compare previous work on ℓ Car with our own observations. Rodgers & Bell (1968) made a study of the $H\alpha$ line in ℓ Car and presented profiles at 18 different phases, they used the same telescope and spectrograph 32-inch (81-cm) camera at Mt. Stromlo that we used, but with a lower dispersion (10Å/mm compared to 2Å/mm). Their data cover two sections of the pulsation cycle, phases 0.94–0.08 and 0.49–0.73. In the first section, their profiles are similar to ours and show the weak red-shifted emission starting between phases 0.0 and 0.08 (see Figure 4.4) but there is no evidence for any residual blue-shifted emission at phase 0.94 in their data. In the other section, there are more discrepancies between the two sets of observations. Again, there is no evidence for a blue-shifted emission in their data but they do not have any observations between

Table 4.2 Summary of some spectral features in ℓ Car

Feature	Phases	Ref. / Notes
H α emission:		this chapter
red-shifted	0.0–0.5	peak at 0.25
blue-shifted	0.6–0.95	peak at 0.9
Mg II emission:		Böhm-Vitense & Love (1994)
stronger red wing	0.1–0.65	
stronger blue wing	0.7–0.1	
metal absorp. lines:		Taylor et al. (1997)
red-shifted	0.40–0.93	
blue-shifted	0.93–0.40	

phases 0.85 and 0.9 when we observed the blue-shifted emission to be strongest. The differences between our observations and theirs may be due to the dispersion, the data recording device (CCD vs photographic plate) or to an intrinsic change in the star.

Böhm-Vitense & Love (1994) made a study of ℓ Car in the UV using the International Ultraviolet Explorer (IUE). They studied the emission-line fluxes of several spectral lines (C II, C IV, Mg II, O I) as a function of pulsational phase. It is interesting to compare the Mg II emission with the H α emission. The Mg II *h* and *k* line profiles consist of a strong emission component, which is effectively split into red and blue wings by a strong absorption component, producing a double hump appearance. The absorption component is stationary and is attributed to circumstellar gas. The overall flux of the emission changes throughout the pulsational cycle. Between phases 0.8 and 0.9 a very steep increase in flux occurs which they suppose is due to an outward-propagating shock. As well as the overall flux of the Mg II emission changing, the relative strength of the two wings also changes, but this variation is 0.1–0.15 cycles out of phase with our observed H α emission shifts (see Table 4.2).

Table 4.2 shows that the H α emission is approximately half a cycle out of phase with the motion of the photosphere as seen from the metal absorption lines. This implies that the emitting gas is travelling in the opposite direction to the photosphere. One possible explanation is that we are seeing moving gas in a shockfront on the far side of the star, this is possible if the radius of the emitting shock is much larger than the photosphere. In this model, the emission from the shockfront on the near side would be obscured by another absorption component, moving nearly in phase with the photosphere, other than the central component due to the circumstellar gas. Another explanation is that there is fairly stable emission from the upper atmosphere. This would arise from the limb and because of projection effects would have almost no Doppler amplitude. An absorption component moving back and forward obscures part of the emission feature creating the red and blue wings. In either case, the H α absorption velocity (not the circumstellar component) is in

the opposite direction to the emission. This means that the $H\alpha$ absorption is red-shifted between phases 0.6–0.95 and blue-shifted from 0.0–0.5 which gives it a phase lag of ~ 0.1 behind the metal line velocity. This is consistent with this $H\alpha$ absorption component being formed higher up in the atmosphere than the metal lines. Further theoretical work may indicate the origin of the $H\alpha$ emission in ℓ Car.